Journal of Hazardous Materials 170 (2009) 735–743

Contents lists available at ScienceDirect

Journal of Hazardous Materials

journal homepage: www.elsevier.com/locate/jhazmat

Modeling of chromium (VI) biosorption by immobilized *Spirulina platensis* in packed column

S.V. Gokhale, K.K. Jyoti, S.S. Lele*

Department of Food Engineering and Technology, Institute of Chemical Technology, Deemed University, Nathalal Parekh Marg, Matunga (E), Mumbai 400019, India

ARTICLE INFO

Article history:
Received 28 September 2008
Received in revised form 2 May 2009
Accepted 6 May 2009
Available online 14 May 2009

Keywords:
Immobilization
Spirulina
Biosorption
Chromium (VI)
Packed bed column
Modeling

ABSTRACT

This study describes biosorption of chromium (VI) by immobilized *Spirulina platensis*, in calcium alginate beads. Three aspects *viz.* optimization of bead parameters, equilibrium conditions and packed column operation were studied and subsequently modeled. Under optimized bead diameter (2.6 mm), calcium alginate concentration (2%, w/v) and biomass loading (2.6%, w/v) maximum biosorption was achieved. 140 g l^{-1} loading of optimized beads resulted in 99% adsorption of chromium (VI) ions from an aqueous solution containing 100 mg l^{-1} of chromium (VI). The quantitative chromium (VI) uptake was effectively described by Freundlich adsorption isotherm. The immobilized *S. platensis* beads were further used in a packed bed column wherein the effects of bed height, feed flow rate, inlet chromium (VI) ion concentration were studied by assessing breakthrough time. The performance data were tested for various models fitting in order to predict scale up-design parameters such as breakthrough time and column height. Results were encouraging.

1. Introduction

Chromium (VI) is a hazardous heavy metal found in industrial effluents of electroplating and leather tanning industries. Biosorption, which utilizes dead biomass of algae, fungi or bacteria to sequester toxic heavy metals, is a well known method for the removal of heavy metals from waste waters. Several metal uptake studies focused on brown marine algae, owing to their high metal adsorption potential, have been carried out [1,2]. However, other algae, such as the green and the blue-green algae, have also been explored for biosorption of heavy metals in this field [3–5]. Gokhale et al. [6] have shown that biosorption using different species of green algae is similar and the biosorption process is "species independent". *Spirulina platensis*, a blue-green alga, was selected for the current study since this alga is relatively cheap and can be easily grown in non-sterile conditions, at an alkalinity of pH 9.5. The probability of contamination under such extreme conditions is very low that offers an added advantage for algal cultivation. This interesting finding will be useful for industrial application after collecting data on technological aspects, such as possible reuse of biomass, e.g. by immobilization, kinetics of process, appropriate bioreactor design—may be packed or fluidized bed, etc. This paper reports further work on chromium (VI) biosorption on *S. platensis* cells immobilized in calcium alginate, using a packed bed column to get performance data for scale up.

Immobilization of biomass using biopolymeric matrices for biosorption has been investigated by many researchers [7–9]. These matrices being effective, non-toxic and inexpensive, offer an economical alternative to ion exchange resins which are routinely used as supports. Calcium alginate, a biopolymer, commercially produced from brown algae, is one such biopolymeric matrix. In the present work calcium alginate gel was used for immobilization of *S. platensis* by the entrapment technique. These gel beads are sensitive to stirring and break when used in mixed flow tanks hence the use of packed column in our current studies. Further, aspects studied were optimization of bead parameters, equilibrium studies and packed column operation modeling. We assume that the following is the first study to report the effect of bead parameters such as bead size, calcium alginate concentration, biomass loading and mechanical strength on biosorption. Hence optimizing these parameters for obtaining efficient biosorption was essential. Equilibrium studies were carried out to measure chromium (VI) adsorption capacity of the biomass. The process engineering advantages of a packed bed adsorption column with immobilized biomass offer ease of scalability and scale up is an important aspect of the biosorption process. Packed bed column studies including effect of bed height, flow rate and initial metal ion concentration on biosorption of chromium (VI). Modeling of data available from column studies facilitates scale-up potential. There are few reports on the modeling of packed bed column using immobilized microalgae for biosorption of heavy metal ions [10,11]. Hence, several models, namely Thomas, Yoon–Nelson,

* Corresponding author. Tel.: +91 22 2414 56 16; fax: +91 22 2414 56 14.
E-mail address: sslele@udct.org (S.S. Lele).

0304-3894/$ – see front matter © 2009 Elsevier B.V. All rights reserved.
doi:10.1016/j.jhazmat.2009.05.005

Nomenclature

a_{mdr}, b_{mdr}	Modified dose–response model constants
C	concentration of chromium (VI) ion in the fluid at any time t (mg l^{-1})
C_0	initial/inlet metal ion concentration (mg l^{-1})
C_b	breakthrough metal ion concentration (mg l^{-1})
C_{eq}	concentration of adsorbate in the fluid at equilibrium (mg l^{-1})
dC/dt	slope of breakthrough curve from t_b to t_e (mg l^{-1} h^{-1})
F	volumetric flow rate (ml h^{-1})
k	first order rate constant (min^{-1})
K_a	adsorption rate constant (l mg^{-1} h^{-1})
K_F	Freundlich adsorption constant
k_{TH}	Thomas model rate constant (mg^{-1} h^{-1})
k_{YN}	Yoon–Nelson model rate constant (min^{-1})
M	biosorbent mass (g)
n	Freundlich adsorption constant
N_0	sorption capacity of bed (mg l^{-1})
q_{eq}	mass of metal ion adsorbed per unit mass of original adsorbent at equilibrium (mg g^{-1})
q_t	mass of metal ion adsorbed per unit mass of original adsorbent at any time t (mg g^{-1})
Q_0	maximum solid-phase concentration of the solute (mg g^{-1})
t	time
t_b	breakthrough time (min)
t_e	exhaustion time (min)
v	linear velocity of solution in the column (cm h^{-1})
V_B	breakthrough volume (l)
V_{eff}	volume of metal solution passed into the column (l)
V_E	exhaust volume (l)
V_R	retention volume (l)
W	total amount of the metal loaded to the column (mg)
W_{ad}	metal ions adsorbed in the column (mg)
Z	column height (cm)
τ	time required for 50% adsorbate breakthrough (min)

Modified dose–response and Bed Depth Service Time (BDST) were investigated in the current study. The first three models predict the service time for a given metal ion concentration and the information thus obtained is useful in the BDST model to predict bed height. The models may also be used for the scale up of the biosorption process. The continuous process for biosorption is proposed at the end.

2. Materials and methods

2.1. Microorganism and growth conditions

The microalga used in the study was *S. platensis* (Strain no.: ARN 740), obtained from CFTRI (Mysore, India). It was maintained in modified Zarrouks medium with analytical grade reagents obtained from Merck [12]. The medium had following composition in g l^{-1}: $NaHCO_3$, 10.08; NaCl, 0.6; $NaNO_3$, 1.5; EDTA disodium magnesium salt, 0.048; K_2SO_4, 0.4; $FeSO_4{\cdot}7H_2O$, 0.004; $CaCl_2$, 0.016; $MgSO_4{\cdot}7H_2O$, 0.08; K_2HPO_4, 0.2; H_3BO_3, 0.00286; $MnCl_2{\cdot}4H_2O$, 0.00181; $ZnSO_4{\cdot}7H_2O$, 0.000222; $Na_2MoO_4{\cdot}2H_2O$, 0.000039; $CuSO_4{\cdot}5H_2O$, 0.000079; $Co(NO_3)_2{\cdot}6H_2O$, 0.000049. *S. platensis* was grown in a 30 l airlift reactor for 15 days under illumination, with an average light intensity of 1500 lx, at room temperature (30 ± 2 °C). Air was sparged at an average flow rate of 6 l min^{-1}. Our earlier studies indicate that aeration of 1 h in every 6 h (4 h in 1 day) results in maximum growth of *S. platensis* (unpublished work); the same was adopted in the present study.

2.2. Chemicals

Chromium (VI) metal ion solution was prepared by diluting stock solution of the concentration 1 g l^{-1} to desired concentrations. Weighed quantities of analytical grade potassium dichromate (obtained from Hi-Media) dissolved in distilled water were used as stock solution. Calcium alginate beads were made by precipitation, on reacting sodium alginate with calcium chloride (both obtained from Hi-Media).

2.3. Analysis of chromium (VI) ions

The concentration of unadsorbed chromium (VI) ions in the biosorption medium was determined spectrophotometrically using diphenyl carbazide as the complexing agent [13] using a Thermo Electron Corporation: Spectronic Genesis 5 spectrophotometer. Optical density was measured at 540 nm with distilled water as a blank.

2.4. Immobilization of S. platensis

Immobilization of algal cells was carried out by the entrapment method. The technique involves drop wise addition of cells suspended in sodium alginate solution into calcium chloride solution, whereon the cells are immobilized in precipitated calcium alginate gel in the form of beads [14].

After the growth phase, the algal culture was centrifuged at 7000 rpm for 15 min, washed with distilled water and dried at 60 °C for 24 h before use. Measured amounts of dry *S. platensis* biomass were suspended in distilled water (4–52 g l^{-1}) and mixed with equal volumes (1:1, v/v) of 4% (w/v) sodium alginate solution (unless otherwise stated). A 100 ml aliquot of sodium alginate-cell suspension was added drop wise to 1000 ml of 10% $CaCl_2$ using a syringe pump. Sodium alginate drops precipitated upon contact with $CaCl_2$, forming gel beads, entrapping the algae cells. These beads were then soaked in $CaCl_2$ solution for 4 h to complete the gelling and were then washed with saline (0.85% NaCl) to remove excessive calcium ions and cells.

2.5. Optimization of bead parameters

The experiments were conducted in 250 ml Erlenmeyer flasks containing 100 ml of chromium (VI) synthetic solution contacted with 10 g of immobilized *S. platensis* beads (unless otherwise stated). The optimum pH for biosorption of chromium (VI) on *S. platensis* was found to be 1.5 [6]. The same was used in the current study. The flasks were agitated at 180 rpm on a rotary shaker. Samples of sorbent suspensions were withdrawn initially at an interval of 20 min for the determination of initial rate, and then at equilibrium (4 h) to determine the residual concentration of metal ions in the solution. The equilibrium results are given in terms of the units of adsorbed metal ion concentration at equilibrium ($C_{ad,eq}$: mg l^{-1}), mass of metal ion adsorbed per unit mass of original biosorbent at equilibrium (q_{eq}: mg g^{-1}), unadsorbed chromium (VI) ion concentration in solution at equilibrium (C_{eq}: mg l^{-1}).

The effects of bead size, biomass loading and calcium alginate concentration on biosorption of chromium (VI) ions were studied. This was done by (i) varying the bead size from 1.9 to 5 mm (±0.2 mm) by using different aperture sizes of the syringe pump; (ii) biomass loading (dry *Spirulina* biomass) was varied from 0.2% to 2.6% (w/v) of sodium alginate solution. Beyond 2.6%, dry *Spirulina* cell mass does not mix well with sodium alginate solution and settles down. (iii) Sodium alginate concentration was varied from 1%

to 6% (w/v). Beyond 6%, the sodium alginate solution becomes very viscous and beads formation through the syringe pump becomes difficult.

The mechanical strength of the beads was checked at each step of optimization using a texture analyzer (Stable Microsystems TXT2i Texture analyzer). Such strength studies are important for designing packed columns, as the strength of the beads is decisive for the height of column. The test parameters were as follows: probe used: P5 (5 mm cylindrical probe); pretest speed: 1 mm s^{-1}; test speed: 0.5 mm s^{-1}; post-test speed: 5 mm s^{-1}; distance: 0.5 mm; acquisition rate: 200 pps. Strength of the beads was measured in gram force at which bead was just about to crush.

2.6. Kinetic and equilibrium studies

In order to study the mechanism of the biosorption process, kinetic models of biosorption are important to analyze experimental data. The widely used models are pseudo first and second order kinetic models. Previously optimized beads were used for this study. In these experiments, 10 g of beads were contacted to 100 ml chromium (VI) ion solution of concentration 100 mg l^{-1}. Samples were taken at 0, 1, 2, 3, 4, 5, 7.5, 10, 12.5, 15, 17.5, 20, 25, 30, 40, 50, 60, 75, 90, 105, 120 min and analyzed for chromium (VI) ion concentration.

Equilibrium experiments consisted of studying adsorption of chromium (VI) ions on immobilized *S. platensis* and fitting the data obtained into various adsorption isotherms. Optimized beads were used for these equilibrium studies. In these experiments, beads were contacted to chromium (VI) ion solution in varying quantities (4, 8, and 12 g per 100 ml). Chromium (VI) ion concentration in the solution was varied as 100, 150, 200 mg l^{-1}. The flasks were rotated on a shaker at 180 rpm for 4 h and the samples were analyzed for residual chromium (VI) ions in solution.

2.7. Packed bed column studies

Continuous biosorption experiments were conducted in a glass column (2 cm ID and 35 cm height), packed with a known quantity of calcium alginate beads. A known concentration of chromium (VI) solution was pumped through the column, at desired flow rates, using a submersible pump. Again, optimized beads were used for the column studies. The void fraction of the bed was 0.46, while the pH of the solution was maintained at 1.5 [6]. Eluent samples were collected every 3 min and were analyzed for chromium (VI) concentration.

The total quantity of metal ions adsorbed in the column (W_{ad}) is calculated from the area over the breakthrough curve (outlet metal concentration vs. time) multiplied by flow rate. Dividing W_{ad} by biosorbent mass (M) leads to the uptake capacity (q) of the biomass. The total amount of the metal ions entering the column can be calculated from the equation:

$$W = \frac{C_0 \cdot F \cdot t_e}{1000} \quad (1)$$

where C_0 is the inlet metal ion concentration (mg l^{-1}), F is the volumetric flow rate (ml h^{-1}) and t_e is the exhaustion time (h).

Total metal removal (%) can be calculated from the equation:

$$\text{total metal removal}\,(\%) = \frac{W_{ad}}{W} \times 100 \quad (2)$$

The effects of the following column parameters, on biosorption of chromium (VI) ions were investigated. (i) Effect of bed height: bed height was varied between 15, 22 and 28 cm, keeping flow rate and initial metal ion concentration constant at 3.5 ml min^{-1} and 100 mg l^{-1}, respectively. (ii) Effect of flow rate: flow rate was varied between 3.5, 7 and 12 ml min^{-1}, while bed height and inlet chromium (VI) ion concentration were held constant at 28 cm and 100 mg l^{-1}, respectively. (iii) Effect of inlet metal ion concentration: inlet concentration of the chromium (VI) ions was varied between 100, 150 and 200 mg l^{-1}, at 28 cm bed height and 3.5 ml min^{-1} flow rate.

3. Results

Study of biosorption using immobilized *S. platensis* consists of two parts: batch studies and packed bed column studies. In batch studies, the immobilization process was optimized followed by kinetic and equilibrium studies. In packed bed column studies breakthrough curves were studied at different operating conditions followed by the modeling of the same.

At this point, it is essential to understand that chromium may exist as chromium (VI) or may get reduced to chromium (III) or even chromium metal. It is reported that chromium (VI) is the most hazardous form due to its mutagenic and carcinogenic properties [15] and chromium metal is the least harmful. The discharge limits involve chromium (VI) and total chromium permissible, e.g. the maximum allowable level for chromium (VI) in domestic water supplies is 0.05 mg l^{-1}, while total chromium, including chromium (III), chromium (VI), and its other forms, is regulated to below 2 mg l^{-1}. The present work involved acidic pH (as low as 1.5 ± 2) where chromium (VI) would not get reduced to chromium (III) [13]. Further, it is reported that during biosorption using *S. platensis*, less than 12% of chromium (VI) was converted to chromium (III) [16]. It is also observed that *S. platensis* has higher adsorption capacity for chromium (III) ($92 \pm 5\%$) than that for chromium (VI) ($75 \pm 5\%$) [16]. Preliminary experiments were conducted where adsorbed chromium (VI) (about 73 mg l^{-1}) was leached out and estimated value was 60 mg l^{-1}. Initial feed had 100 mg l^{-1} of chromium (VI) and hence our findings were in line with other reports. In view of above the subsequent work was carried out for packed bed studies assuming that entire chromium (VI) added existed in the same oxidative state.

3.1. Batch studies

Batch studies consisted of two parts: (i) optimization of immobilization process and (ii) kinetic and equilibrium studies of biosorption. *S. platensis* immobilized in calcium alginate beads by the entrapment method was used for biosorption of chromium (VI) ions. It was observed (from Table 1) that 140 g of beads are required to almost completely remove chromium (VI) ions from the solution of concentration 100 mg l^{-1}. These 140 g beads contain 9.5 g of dry *S. platensis* biomass. When free *S. platensis* cells were used, only 2.4 g of dry biomass was required to treat same chromium (VI) solution.

For optimization of immobilization parameters, the effects of bead size, biomass loading and calcium alginate concentration on

Table 1
Comparison of the equilibrium adsorption yields for immobilized and free cells of microalgae at different biosorbent concentration.

Immobilized cells			Free cells	
M (g l^{-1})	X_{im} (g l^{-1})	% Ad	X_f (g l^{-1})	% Ad
20	1.36	30.78	1.2	73.64
40	2.71	54.66	1.4	78.18
60	4.07	68.63	1.6	83.18
80	5.43	78.54	1.8	88.64
100	6.78	86.23	2	92.73
120	8.14	93.51	2.2	98.64
140	9.50	99.22	2.4	99.53

C_0: 100 mg l^{-1}; temperature: 25 °C; agitation rate: 180 rpm. Where M is mass of beads contacted with the chromium (VI) solution (g l^{-1}); X_{im} is the mass of immobilized microalgal cells (mg l^{-1}); and X_f is mass of free microalgal cells (mg l^{-1}).

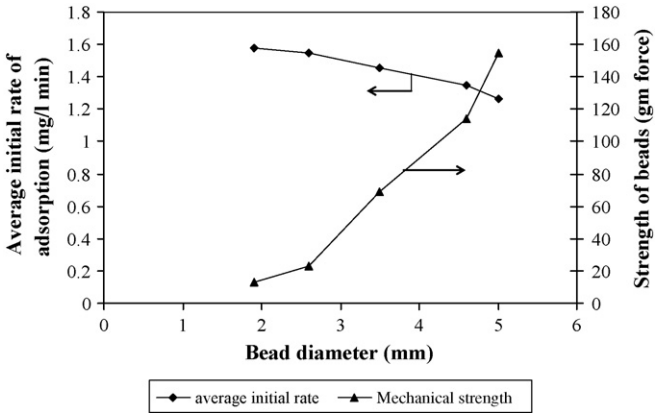

Fig. 1. Effect of bead size on biosorption of chromium (VI) ions (C_0: 100 mg l^{-1}, biomass loading: 10.0 g l^{-1}, calcium alginate concentration: 2% (w/v), temperature: 30 °C, pH: 1.5, and agitation rate: 180 rpm).

biosorption of chromium (VI) ions were studied. The first step was to study effect of bead size. When the bead size was varied between 1.9 and 5 mm, the average initial rate of adsorption decreased (Fig. 1). However, equilibrium adsorption of chromium (VI) ions was almost equal (approximately 56 mg l^{-1}) for all bead sizes. The second step was to see the effect of biomass loading, which also plays an important role in biosorption. As biomass loading was increased from 0.2% to 2.6% (w/v), an increase in equilibrium biosorption was observed up to a certain critical biomass loading value (2.2%) which then plateaus off (Fig. 2). The final step was to study the effect of calcium alginate concentration. When calcium alginate concentration increased from 1% to 6% (w/v), the equilibrium biosorption of chromium (VI) ions decreased from 95.49 to 85.41 g l^{-1} (Fig. 3).

Another critical factor affecting the column design is the mechanical strength of the beads, which was found to be considerably affected by bead size and calcium alginate concentration. As bead size increased from 1.9 to 5 mm, bead strength increased from 13.33 to 154.48 g force (Fig. 1). With an increase in calcium alginate concentration from 1% to 6% (w/v), mechanical strength of the beads increased from 18.8 to 35.6 g force (Fig. 3).

Based on the above observations, following bead parameters were selected for equilibrium batch studies and packed column studies:

Bead size	2.6 mm
Biomass loading	2.6% (w/v)
Calcium alginate concentration	2% (w/v)

The data of variation of chromium (VI) metal ion concentration in solution with time was collected. Pseudo first order model

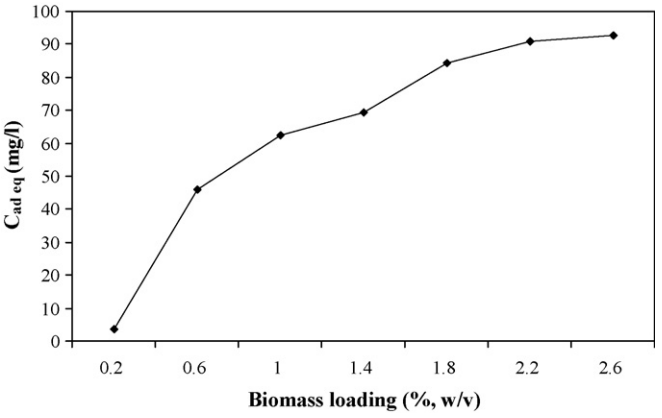

Fig. 2. Effect of biomass loading in beads on equilibrium biosorption of chromium (VI) ions (C_0: 100 mg l^{-1}, bead diameter: 2.6 mm, calcium alginate concentration: 2% (w/v), temperature: 30 °C, pH: 1.5, and agitation rate: 180 rpm).

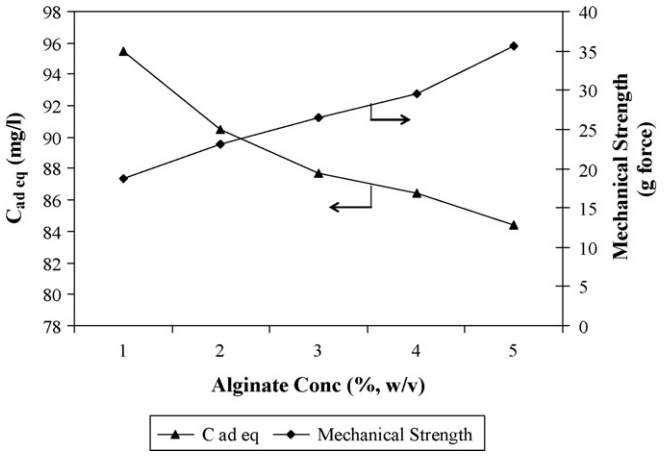

Fig. 3. Effect of calcium alginate concentration on biosorption of chromium (VI) ion concentration (C_0: 100 mg l^{-1}, bead diameter: 2.6 mm, biomass loading: 26 g l^{-1}, temperature: 30 °C, pH: 1.5, and agitation rate: 180 rpm).

was used to fit the experimental kinetic data. The mathematical expressions for the model is given as

$$\ln(q_e - q_t) = \ln q_e - kt \quad (3)$$

where q_e is equilibrium chromium (VI) uptake (mg g^{-1}), q_t is amount of chromium (VI) ions adsorbed on the algal biomass at any time t, k (min^{-1}) is the first order rate constant. The first order adsorption rate constant, k for chromium sorption was calculated from the slope of the linear plot of $\ln(q_e - q_t)$ vs. time. In the current study, samples were taken at various time intervals between 1 and 120 min. Biosorption capacity increases with time. The first order rate constant k was found to be 0.0236 min^{-1} and correlation regression coefficient, $R^2 = 0.97$.

Equilibrium relationship between the concentration of metal ions in the fluid phase and the concentration of adsorbed metal ions at a constant temperature is represented by an adsorption isotherm. There are several adsorption isotherm expressions available *viz.* Freundlich isotherm, Langmuir isotherm, BET isotherm, etc. Data obtained in the current study fitted well to the Freundlich adsorption isotherm. The Freundlich adsorption isotherm gives the empirical relation between the q_{eq} and the C_{eq}. The Freundlich isotherm is given by the relation:

$$q_{eq} = K_F \cdot C_{eq}^{n} \quad (4)$$

where q_{eq} is adsorbate loading at equilibrium (mg g^{-1}), C_{eq} is the concentration of adsorbate in the fluid at equilibrium (mg l^{-1}), and K_F is the Freundlich adsorption constant. Experimental data of chromium (VI) biosorption on immobilized *S. platensis* gel beads were fitted to linearized Freundlich model to evaluate the model constants (K_F and n). Eq. (4) was linearized as

$$\ln q_{eq} = \ln K_F + n \ln C_{eq} \quad (5)$$

Plot of $\ln q_{eq}$ vs. $\ln C_{eq}$ gives straight line with intercept as $\ln K_F$ and slope as n (Fig. 4).

The Freundlich adsorption constants evaluated from the linearized model and the regression correlation coefficient are as follows: $K_F = 9.14$; $n = 0.25$; $R^2 = 0.91$.

It is interesting to note that the standard model for adsorption has shown good fit to the data supporting that most of the chromium (VI) was indeed adsorbed rather than chemically changing the oxidative state, or in the free form.

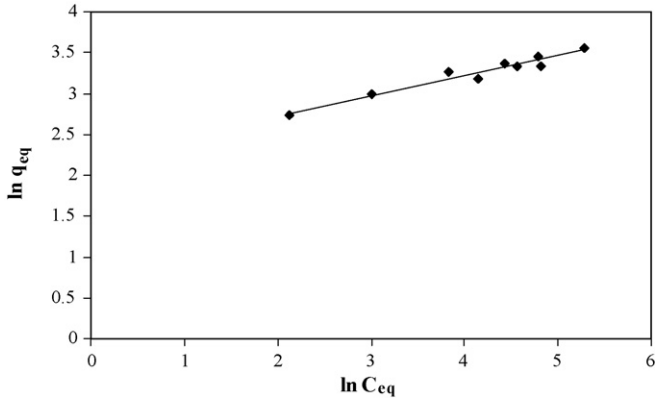

Fig. 4. The linearized Freundlich adsorption isotherm of chromium (VI) by calcium alginate beads at 30 °C: (♦) experimental data (—) Freundlich model predicted data (C_0: 100 mg l^{-1}, X: 26 g l^{-1}, temperature: 30 °C, pH: 1.5, and agitation rate: 180 rpm).

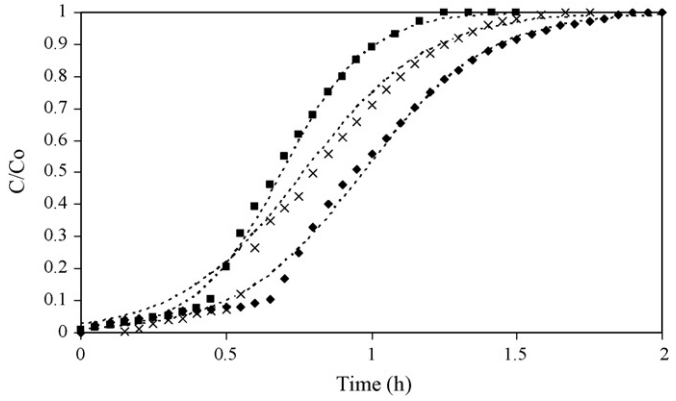

Fig. 5. Breakthrough curve for chromium (VI) biosorption onto *S. platensis*-Ca-alginate beads at different bed heights. Bed height, flow rate and inlet concentration (♦) 28 cm, 3.5 ml/min, 100 mg l^{-1}, (×) 22 cm, 3.5 ml/min, 100 mg l^{-1}, (■) 15 cm, 3.5 ml/min, 100 mg l^{-1} (F: 3.5 ml h^{-1}, C_0: 100 mg l^{-1}, temperature: 30 °C, and influent pH: 1.5).

3.2. Packed bed column studies

Column operations do not have sufficient contact time for attainment of equilibrium. Hence, in addition to equilibrium studies, there was a need to perform biosorption studies using a column. Effect of various column parameters on biosorption rates was investigated.

Fig. 5 shows the plot of C/C_0 vs. t (breakthrough curve) at different bed heights. Figure also shows the Thomas model predicted curves obtained by nonlinear regression. Table 2 gives the chromium (VI) uptake, breakthrough and exhaustion time. The chromium (VI) uptake capacity of beads remained almost similar for different bed heights (Table 2). The breakthrough time (t_b,) and exhaustion time (t_e) increased with increase in bed height. The slope of the S-curve from t_b to t_e (dC/dt) in Fig. 5 decreased as the bed height increased from 15 to 28 cm, indicating that breakthrough curve becomes steeper as the bed height decreases.

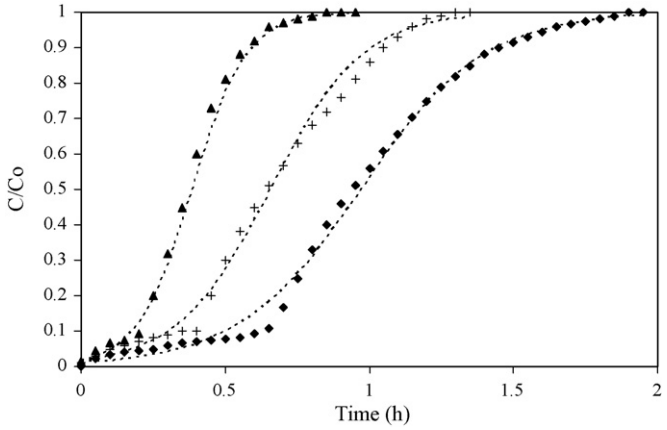

Fig. 6. Breakthrough curve for Chromium (VI) biosorption onto *S. platensis*-Ca-alginate beads at different flow rates. Bed height, flow rate and inlet concentration (♦) 28 cm, 3.5 ml/min, 100 mg l^{-1}, (+) 28 cm, 7 ml/min, 100 mg l^{-1}, (▲) 28 cm, 12 ml/min, 100 mg l^{-1} (Z: 28 cm, C_0: 100 mg l^{-1}, temperature: 30 °C, and influent pH: 1.5).

The breakthrough curves obtained by varying flow rates from 3.5 to 12 ml h^{-1}, at column height of 28 cm bed height and 100 mg l^{-1} of inlet metal ion concentration are shown in Fig. 6. At the lowest flow rate (3.5 ml min^{-1}), a typical S-shaped breakthrough curve was seen. As the flow rate increased, the breakthrough curves became steeper. Almost 56% of chromium (VI) ions were removed at the lowest flow rate (3.5 ml min^{-1}) as compared to 44% at higher flow rates (12 ml min^{-1}) as seen from Table 2.

An important parameter that affects biosorption rates is the initial metal ion concentration. The lowest inlet chromium (VI) ion concentration (100 mg l^{-1}) resulted in a delayed breakthrough curve (Fig. 7). As the inlet chromium (VI) ion concentration increased, much sharper breakthrough curves are seen. Taking the columns biosorption performance into account, the highest inlet chromium (VI) ion concentration resulted in decreased chromium (VI) removal (Table 2).

To describe the column breakthrough curves obtained at different bed heights, flow rates and inlet metal concentrations, three models were used. These include:

Thomas model

$$\frac{C}{C_0} = 1 + \exp\left(\frac{k_{TH}}{F}(Q_0 M - C_0 V_{eff})\right) \quad (6)$$

Yoon–Nelson model

$$\frac{C}{C_0} = \frac{(\exp k_{YN} t - \tau k_{YN})}{1 + (\exp k_{YN} t - \tau k_{YN})} \quad (7)$$

Modified dose–response model

$$\frac{C}{C_0} = 1 - \frac{1}{1 + (V_{eff}/b_{mdr})^{a_{mdr}}} \quad (8)$$

Table 2
Column data and parameters obtained at different bed heights, flow rates and inlet concentrations.

Bed height (cm)	Mass of beads (g)	Flow rate (ml h^{-1})	C_0 (mg l^{-1})	q (mg g^{-1})	t_b (min)	t_e (min)	dC/dt (mg l^{-1} min^{-1})	Cr (VI) removal (%)
15	42	3.5	100	354.25	27	75	2.4	56.68
22	59	3.5	100	297.11	33	100	5.25	50.93
28	59	3.5	100	260.38	39	114	5.31	49.59
28	59	7	100	370.01	24	78	7.5	46.50
28	59	12	100	372.27	12	51	12	44.38
28	59	3.5	150	203.46	30	84	8.0	35.06
28	59	3.5	200	150.82	21	69	10.8	23.73

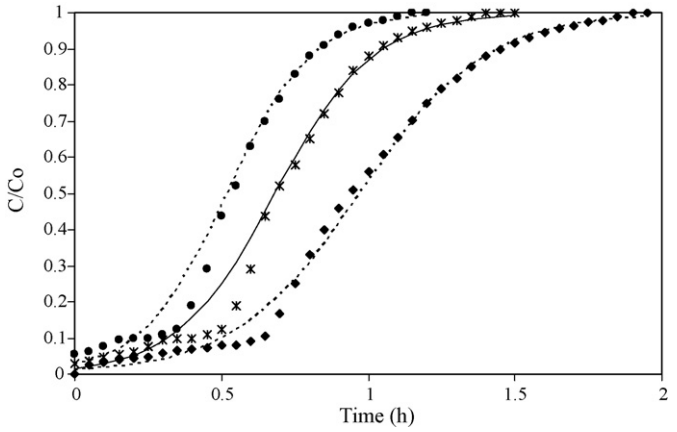

Fig. 7. Breakthrough curves for chromium (VI) biosorption onto *S. platensis*-Ca-alginate beads at different inlet chromium (VI) ion concentrations. Bed height, flow rate and inlet concentration (♦) 28 cm, 3.5 ml/min, (*) 28 cm, 3.5 ml/min, 150 mg l^{-1}, (●) 28 cm, 3.5 ml/min, 200 mg l^{-1} (*Z*: 28 cm, *F*: 3.5 ml h^{-1}, temperature: 30 °C, and influent pH: 1.5).

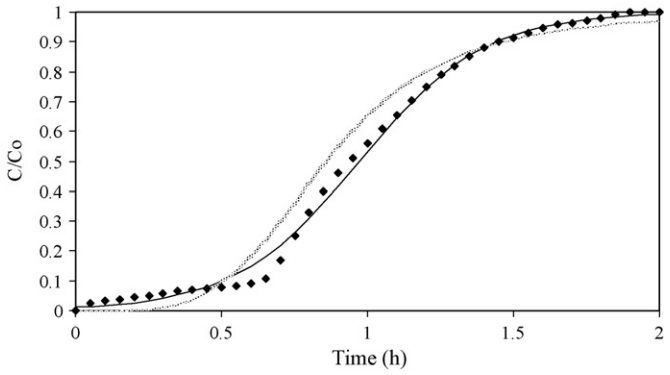

Fig. 8. Prediction of breakthrough curve data by Thomas model, Yoon–Nelson model and Modified dose–response model: (♦) experimental data, (—) predicted by Thomas model, (- - - -) predicted by Yoon–Nelson model, (···) predicted by Modified dose–response model (bed height: 28 cm, flow rate: 3.5 ml min^{-1}, initial chromium (VI) ion concentration: 100 mg l^{-1}, temperature: 30 °C, and influent pH: 1.5).

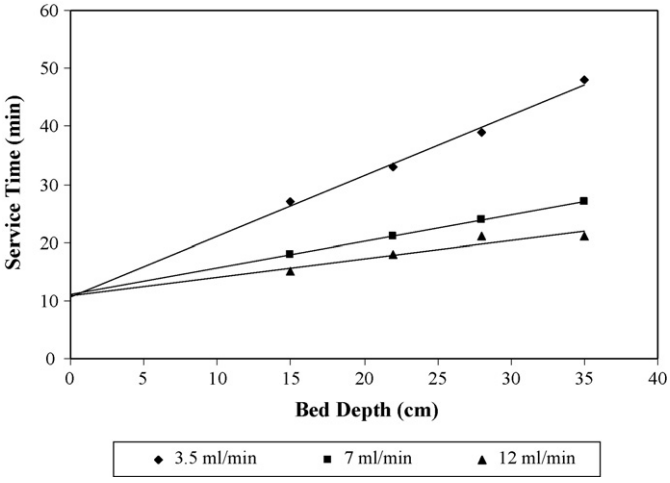

Fig. 9. BDST model plot for chromium (VI) biosorption on microalgae-Ca-alginate beads at different flow rates (inlet chromium (VI) ion concentration: 100 mg l^{-1}, temperature: 30 °C, and influent pH: 1.5).

where k_{TH} is the Thomas model rate constant (mg^{-1} h^{-1}), F is the flow rate of the stream passing through column (l/min), Q_0 is the maximum solid-phase concentration of the solute (mg g^{-1}), V_{eff} is the volume of metal solution passed into the column (l), k_{YN} is the Yoon–Nelson model rate constant (min^{-1}), τ is the time required for 50% adsorbate breakthrough (min) and a_{mdr} and b_{mdr} are the Modified dose–response model constants.

These models predict the service time for a given metal ion concentration. Experimental data obtained from column studies were fitted to the three models described here. Best fits were obtained with Thomas model and Yoon–Nelson model as shown in Table 3, with correlation regression coefficients (R^2) ranging between 0.97 and 0.99, as compared to those obtained for Modified dose–response model (R^2 ranging between 0.92 and 0.95). The breakthrough curves predicted by all the three models for column biosorption data at optimum bed height (28 cm), flow rate (3.5 ml min^{-1}) and initial chromium (VI) concentration (100 mg l^{-1}) are shown in Fig. 8. The model constants for different bed heights, flow rates and initial chromium (VI) ion concentration are given in Table 3.

After predicting the breakthrough time (service time) for the stream with given inlet metal ion concentration the height of the column required can be found using the Bed Depth Service Time (BDST) model. The BDST model states that there is a linear relationship between bed height (Z) and service time (t) of a column. The equation is expressed as

$$t = \frac{N_0 Z}{C_0 v} + \frac{1}{K_a C_0} \ln\left(\frac{C_0}{C_b} - 1\right) \quad (9)$$

where C_b is the breakthrough metal ion concentration (mg l^{-1}), N_0 is the sorption capacity of bed (mg l^{-1}), v is the linear velocity (cm h^{-1}) and K_a is the rate constant (l mg^{-1} h^{-1}). The data of service time against bed height at different flow rates and different inlet chromium (VI) ion concentrations were plotted (Figs. 9 and 10). Eq. (9) implies that the service time is a linear function of the bed height and hence it can be written as

$$t = mZ - n \quad (10)$$

where m is the slope of the BDST line and n is the intercept of the BDST line. For different flow rates, intercept of the graph remains same (Fig. 9), whereas for different inlet metal ion concentration, slop of the graph remains near about same (Fig. 10). Linear correlation coefficients greater than 0.9 show that the BDST model is valid for the present system. The sorption capacity of the bed per

Table 3
Thomas, Yoon–Nelson and Modified dose–response model constants at different bed heights, flow rates and initial chromium (VI) ion concentrations.

Z (cm)	F (ml min^{-1})	C_0 (mg ml^{-1})	Thomas model			Yoon–Nelson model			Modified dose–response model		
			Q_0	k_{TH}	R^2	k_{YN}	τ	R^2	a_{mdr}	b_{mdr}	R^2
15	3.5	100	5.765	0.069	0.99	6.882	0.692	0.99	4.297	2.24	0.95
22	3.5	100	4.996	0.061	0.98	6.111	0.857	0.98	4.378	2.61	0.94
28	3.5	100	4.476	0.047	0.97	4.680	0.972	0.97	4.191	3.01	0.92
28	7	100	6.042	0.062	0.98	6.242	0.656	0.98	4.466	4.29	0.92
28	12.5	100	6.087	0.107	0.99	10.698	0.370	0.99	3.733	3.86	0.92
28	3.5	150	4.716	0.040	0.97	6.003	0.683	0.97	4.806	2.27	0.93
28	3.5	200	4.781	0.035	0.97	6.991	0.519	0.97	4.228	1.69	0.93

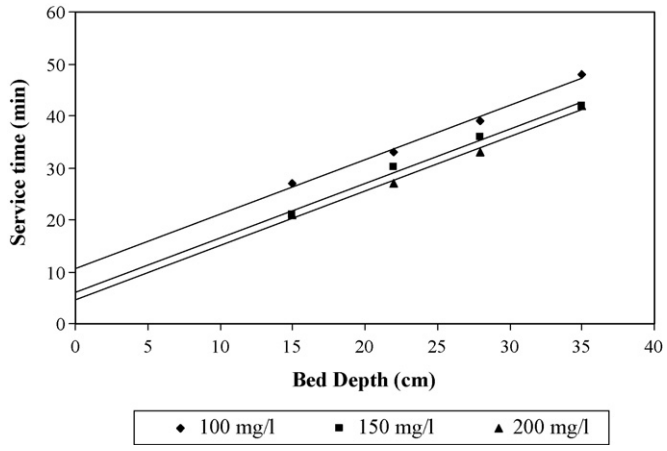

Fig. 10. BDST model plot for chromium (VI) biosorption on microalgae-Ca-alginate beads at different inlet concentrations (flow rate: 3.5 ml min^{-1}, temperature: 30 °C, and influent pH: 1.5).

unit bed volume, N_0 and rate constant K_a were calculated from the slope and intercept of BDST plot, respectively. From Fig. 9, the computed values of N_0 for three flow rates of 3.5, 7, and 12 ml min^{-1} are 116.48, 101.14, and 120.85 mg l^{-1}, respectively with average K_a of 2.02×10^{-3} l mg^{-1} h^{-1}. From Fig. 10, the computed values of K_a for three inlet concentrations of 100, 150, and 200 mg l^{-1} are 2.07×10^{-3}, 2.40×10^{-3}, and 2.39×10^{-3} l mg^{-1} h^{-1}, respectively with average N_0 of 116.48 mg l^{-1}.

4. Discussion

S. platensis immobilized in calcium alginate beads by the entrapment method was used for biosorption of chromium (VI) ions. Free cells are not suitable for use in a column because of their low density and small size, which would result in plugging the bed, resulting in larger pressure drops. The poor mechanical strength, rigidity and solid–liquid separation add to the limitations in the use of free cells [17]. The advantages of immobilized algal biomass are manifold. Firstly, immobilization of cells in solid matrix would give ideal size, mechanical strength, rigidity and porosity necessary for the use in column operations [18,19]. Secondly the demand for algal biomass would be reduced, since immobilized systems can be regenerated easily and reused several times [20]. This reduces the need for mass algal cultivation; which is often the bottleneck encountered in biosorption of heavy metals. This consequently improves process economics. Thirdly, downstream processing is a major factor influencing cost of heavy metal biosorption using free cells. When free cells are used, they have to be separated from solution, generally by centrifugation. But employing immobilized algal beads eliminates routinely used separation techniques and offers an economical alternative [19,21]. Finally, the problems encountered in disposal of toxic sludge generated in the form of immobilized biomass would be greatly reduced as compared to free biomass, since the former would be in a more concentrated form [20]. These factors clearly indicate the potential advantages of employing immobilized biomass.

However there are some limitations of immobilization. From Table 1 it can be seen that compared to free cells, more immobilized cells are required to treat same chromium (VI) ion solution. This is due to higher mass transfer resistance to diffuse chromium (VI) ions in the gel beads and due to the blocking of some active sites on algal cell wall. Although a higher quantity of biomass was required for biosorption using immobilized *S. platensis*, the beads could be regenerated by changing the pH and could be reused at least five times. Thus, effectively less biomass is required in the immobilized state as compared to free cells in order to treat same volumes of chromium (VI) solutions of identical concentrations. This would be clearly advantageous in large scale applications.

4.1. Batch studies

In the first part, optimization of immobilization process, three parameters were studied: (i) bead size: as bead size increases, surface area available for chromium (VI) ion diffusion into the beads decreases, and hence the rate of biosorption decreases. But equilibrium biosorption capacity remains same. This was because an equal mass (5 g) of beads was added to chromium (VI) ion solution for each bead size and as biomass loading and calcium alginate concentration is same for all bead sizes, the density of the bead and hence the amount of beads added to chromium (VI) ion solution also remains the same. (ii) Biomass loading: increased biomass loading provides more active sites for biosorption to occur and hence increases the rate of biosorption. On the other hand, as biomass loading increases, porosity of the beads decreases, resulting in lowering of biosorption rates. Therefore after a critical value, increasing the biomass loading will not be useful. Moreover, dry *Spirulina* biomass does not mix well with sodium alginate beyond a certain limit. Hence, in the present study, biomass loading only up to 2.6% was used. (iii) Calcium alginate concentration: increase in alginate concentration is attributed to decrease in porosity of beads with decrease in biosorption capacity.

Mechanical strength was yet another parameter taken into consideration for optimization of immobilization process. Larger the bead size, higher is the amount of calcium alginate and biomass, which contributes to higher mechanical strength. Thus, rate of adsorption was found to be inversely proportional, while mechanical strength is directly proportional to bead size. Although equilibrium biosorption rate was almost the same for all bead sizes, larger beads exhibited higher mechanical strength which is a desirable feature in column studies. Hence, an optimum bead size of 2.6 mm with mechanical strength of 23.73 g force was selected for column studies which were sufficient for designing a lab scale biosorption column. Increasing calcium alginate concentration gives rise to higher cross-linking within the beads, thus imparting higher mechanical strength to the immobilized beads. The rate of biosorption, is therefore inversely proportional while mechanical strength is directly proportional to the concentration of calcium alginate. An optimum calcium alginate concentration of 2% was selected for the study. Although the biosorption rate obtained with 2% calcium alginate concentration would be less than that obtained with 1%. The mechanical strength of beads with 2% calcium alginate was higher than beads with 1% calcium alginate, 23.1 g force as compared to 18.8 g force respectively. This sufficed for designing a lab scale biosorption column. As the scale of the column is increased, an optimum combination of bead size and calcium alginate concentration should be used.

Biosorption kinetics and equilibrium studies were carried out in the second part. Biosorption is a rapid process and around 50% of the chromium (VI) ions were adsorbed in first 20 min. The rate of adsorption is proportional to the active sites available and the concentration of chromium (VI) ions in the solution. As time lapses, both active sites and chromium (VI) ions go on decreasing which results in decrease in rate of adsorption. Pseudo first order rate model describes the experimental data satisfactorily.

Biosorption of a metal ion depends upon temperature, concentration, nature of metal ion and the nature of biosorbent. That means at a constant temperature, extent of biosorption on a particular biosorbent depends on the concentration of a metal ion and biomass loading. During biosorption, equilibrium is established between adsorbed metal ions on the cell surface and the unadsorbed metal ions in the solution. Adsorption isotherm represents

equilibrium relationship between the concentration of metal ions in the fluid phase and the concentration of adsorbed metal ions. Experimental data fitted well to Freundlich adsorption isotherm.

4.2. Packed bed column studies

Sorption capacity of immobilized *S. platensis*, obtained from batch equilibrium experiments, was useful in providing fundamental information about the effectiveness of the metal-biosorbent system. However, this data may not be applicable to most treatment systems such as column operations, where contact time is not sufficient for attainment of equilibrium. Hence the need to perform biosorption studies using a column. Column studies comprise of studies of breakthrough curves at different bed heights, flow rates, initial metal ion concentration and the modeling of these studies.

Uptake capacity depends mainly upon the amount of biosorbent available for adsorption. The breakthrough time (t_b,) and exhaustion time (t_e) increased with increase in bed height since more time was required to exhaust more beads. The slope of the breakthrough curve from t_b to t_e decreased as the bed height increased. This is due to an increase in axial dispersion of the metal ions over the column with an increase in column height. This increase in bed height resulted in an increase in volume of metal ion solution treated and therefore a higher percentage of chromium (VI) removal.

A delayed breakthrough and exhaustion time resulted in efficient utilization of beads, resulting in better metal uptake. As the flow rate increased, the breakthrough curves became steeper. Relatively early breakthrough and exhaustion times resulted in comparatively less chromium (VI) uptake at higher flow rates. Though biosorption is a very fast process and metal ion removal is mainly controlled by the diffusion of ions into the beads. At higher flow rates diffusion effects are lower due to the insufficient residence time of metal ions in the column. Hence lower flow rates are desirable for effective removal of metal ions.

The lowest inlet chromium (VI) ion concentration resulted in a delayed breakthrough curve since the lower concentration gradient causes reduced transport of the metal ions (Fig. 7). The driving force for biosorption is the concentration difference between the solute on the sorbent and the solute in solution. High concentration differences provide a higher driving force, which favors the biosorption process. Although percentage chromium (VI) removal is lower at high initial metal ion concentrations, sharper breakthrough curve was observed, indicating shortened mass transfer zone and higher biosorption rates. Therefore, when quick metal uptake is desired, which is often the case, operating with high initial metal ion concentrations appears to be favorable.

For modeling of breakthrough curves, three models were used *viz.* Thomas model, Yoon–Nelson model and Modified dose–response model. The Thomas model, based on the Langmuir adsorption–desorption kinetics, is one of the most widely used models [10]. It assumes no axial dispersion and sorption is the rate driving force and obeys second order reversible reaction kinetics [11]. The Yoon–Nelson model is based on the assumption that the rate of decrease in the probability of adsorption for each sorbate molecule is proportional to the probability of sorbate sorption and the probability of sorbate breakthrough on the sorbent [11]. The Modified dose–response model proposed by Yan et al. [22] minimizes the error that results from use of the Thomas model, especially with lower and higher breakthrough curve times. The model constant (a_{mdr}) increases with increasing bed height, decreasing flow rate and decreasing initial metal ion concentration. The Thomas model showed better fit than the other two.

After predicting the breakthrough time the height of the column required can be found out using Bed Depth Service Time (BDST) model. The BDST model, proposed by Bohart and Adams [23] and subsequently modified by Hutchins [24], is based on physically measuring the capacity of the bed at different breakthrough values. The simplified design model ignores the intraparticle mass transfer resistance [25]. The rate constant, K_a, calculated from the intercept of BDST plot, characterizes the rate of solute transfer from the fluid phase to the solid phase [26]. If K_a is large, even a short bed will avoid breakthrough, but as K_a decreases a progressively longer bed

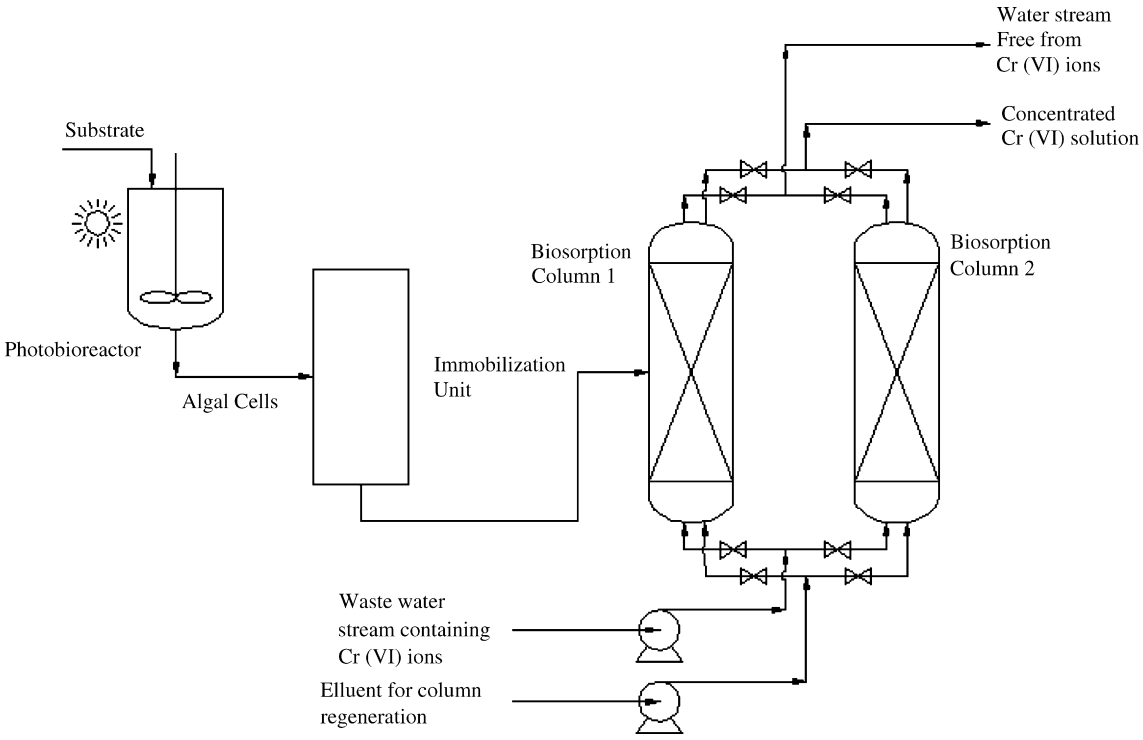

Fig. 11. Proposed flow sheet for continuous operation.

is required to avoid breakthrough [26]. For the present system, very small value of rate constant K_a (2.07×10^{-3} to 1.4×10^{-3} l mg^{-1} h^{-1}) in BDST model indicated that a longer bed would be required to avoid breakthrough.

From the present data, it can also be seen that the BDST equation determined at a given flow rate (v) and inlet solute concentration (C_0) can be modified to predict the BDST equations at different v and C_0. Cooney [26] suggested that the BDST model rate constant (K_a) is not significantly affected by the change in flow rate, and thus the intercept n of Eq. (9) remains essentially unchanged when flow rate is changed. However, the slope m of Eq. (9) does change with change in flow rate and hence given by:

$$\text{new slope} = \text{old slope}\,\frac{v_{\text{old}}}{v_{\text{new}}} \tag{11}$$

In contrary, the change in inlet solute concentration (C_0) usually results in change in slope and intercept of BDST equation. The new slope and intercept values can be determined from:

$$\text{new slope} = \text{old slope}\,\frac{C_{0,\text{old}}}{C_{0,\text{new}}} \tag{12}$$

$$\text{new intercept} = \text{old intercept}\left(\frac{C_{0,\text{old}}}{C_{0,\text{new}}}\right) \times \left(\frac{\ln[(C_{0,\text{new}}/C_b)-1]}{\ln[(C_{0,\text{old}}/C_b)-1]}\right) \tag{13}$$

The advantage of the BDST model is that any experimental test can be reliably scaled up to other flow rates and inlet solute concentrations without further experimental tests [10]. Based on the studies presented here a continuous large scale biosorption process is proposed as shown in Fig. 11. Two biosorption columns can be used alternately such that when biosorption progresses in one column, the beads in other column are being regenerated and vice versa. When biosorption column 1 is fully saturated with chromium (VI) ions (after the break though), the flow is switched over to second column. Thus in these studies, immobilized algal beads were used for continuous packed bed column studies and also different models were used for the same. Thus immobilization technique can be effectively used for continuous biosorption process at larger scale of operation.

5. Conclusion

Immobilized *Spirulina* was effectively used for chromium (VI) removal from aqueous solutions. Bead parameters such as size, calcium alginate concentration and biomass loading had significant effects on the biosorption rate, in addition to their primary effect on the mechanical strength of the beads. The optimum bead parameters for lab scale experiments were: bead size: 2.6 mm, biomass loading: 2.6% (w/v) and calcium alginate concentration: 2% (w/v). The quantitative chromium (VI) uptake by immobilized *S. platensis* was effectively described by Freundlich adsorption isotherm. 140 g l^{-1} of optimized beads containing 9.5 g of dry *Spirulina* biomass resulted in 99% adsorption from an aqueous solution containing 100 mg l^{-1} chromium (VI). Packed columns are preferred configurations for continuous operations and the advantages of immobilized biomass can be effectively realized in packed columns for large scale applications. Packed bed column studies using immobilized *S. platensis* revealed that column performance was significantly affected by bed height, flow rate and initial metal ion concentration. Increasing bed height and flow rate resulted in better utilization of the packed bed and higher biosorption rates. The data indicated that high initial metal ion concentration should be used for quick metal uptake. Modeling column data resulted in best fits with the Thomas model and Yoon–Nelson model; which predict the service time required for a given metal ion concentration. The data also fitted well into the Bed Depth Service Time (BDST) model; which predicts a linear relationship between bed height and service time. For the present system, a very small value of rate constant K_a (2.02×10^{-3} l mg^{-1} h^{-1}) in BDST model indicated that a longer bed would be required to avoid breakthrough. Thus immobilization technique can be effectively used for continuous biosorption process at larger scales of operation.

References

[1] M.M. Figueira, B. Volesky, V.S.T. Cemenelli, F.A. Roddick, Biosorption of metals in brown seaweed biomass, Water Res. 34 (2000) 196–204.
[2] T.A. Davies, B. Volesky, A. Mucci, A review of the biochemistry of heavy metal biosorption by brown algae, Water Res. 37 (2003) 4311–4330.
[3] Z. Aksu, Determination of the equilibrium, kinetic and thermodynamic parameters of the batch biosorption of nickel (II) ions onto *Chlorella vulgaris*, Process Biochem. 38 (2002) 89–99.
[4] K. Chojnacka, A. Chojnacki, H. Gorecka, Biosorption of Cr^{3+}, Cd^{2+} and Cu^{2+} ions by blue-green algae *Spirulina* sp.: kinetics, equilibrium and the mechanism of the process, Chemosphere 59 (2005) 75–84.
[5] G.Ç. Dönmez, Z. Aksu, A. Öztürk, T. Kutsal, A comparative study on heavy metal biosorption characteristics of some algae, Process Biochem. 34 (1999) 885–892.
[6] S.V. Gokhale, K.K. Jyoti, S.S. Lele, Kinetic and equilibrium modeling of chromium (VI) biosorption on fresh and spent *Spirulina platensis*/*Chlorella vulgaris* biomass, Bioresour. Technol. 99 (2008) 3600–3608.
[7] Z. Aksu, G. Eğretli, T. Kutsal, A comparative study of copper (II) biosorption on Ca-alginate, agarose and immobilized *C. vulgaris* in a packed-bed column, Process Biochem. 33 (1998) 393–400.
[8] N. Akhtar, J. Iqbal, M. Iqbal, Removal and recovery of nickel (II) from aqueous solution by loofa sponge-immobilized biomass of *Chlorella sorokiniana*: characterization studies, J. Hazard. Mater. B108 (2004) 85–94.
[9] R. Singh, B.B. Prasad, Trace metal analysis: selective sample (copper II) enrichment on an AlgaSORB column, Process Biochem. 35 (2000) 897–905.
[10] K. Vijayaraghavan, D. Prabu, Potential of *Sargassum wightii* biomass for copper (II) removal from aqueous solutions: application of different mathematical models to batch and continuous biosorption data, J. Hazard. Mater. 137 (2006) 558–564.
[11] Z. Aksu, F. Gönen, Biosorption of phenol by immobilized active sludge in a continuous packed bed: prediction of break though curves, Process Biochem. 39 (2003) 599–613.
[12] G. Mahajan, M. Kamat, γ-Linolenic acid production from *Spirulina platensis*, Appl. Microbiol. Biotechnol. 43 (1995) 466–469.
[13] F.D. Snell, C.T. Snell, C.A. Snell, Colouimetric methods of analysis, vol. II A, third ed., D. Van Nostrand Company Inc., New York, 1959.
[14] A. Rosevear, Immobilized biocatalysts—a critical review, J. Chem. Technol. Biotechnol. 34B (1984) 127–150.
[15] M. Dakiky, M. Khamis, A. Manassra, M. Mer'eb, Selective adsorption of chromium (VI) in industrial wastewater using low cost abundantly available adsorbents, Adv. Environ. Res. 6 (2002) 533–540.
[16] Y. Madrid, M.E. Barrio-Cordoba, C. Cámara, Biosorption of antimony and chromium species by *Spirulina platensis* and *Phaseolus*. Applications to bioextract antimony and chromium from natural and industrial waters, Analyst 123 (1998) 1593–1598.
[17] R. Kumar, R. Singh, N. Kumar, K. Bishnoi, N.R. Bishnoi, Response surface methodology approach for optimization of biosorption process for removal of Cr (VI), Ni (II) and Zn (II) ions by immobilized bacterial biomass sp. *Bacillus brevis*, Chem. Eng. J. 146 (2009) 401–407.
[18] J. Wang, C. Chen, Biosorbents for heavy metals removal and their future, Biotechnol. Adv. 27 (2009) 195–226.
[19] N.R. Bishnoi, R. Kumar, K. Bishnoi, Biosorption Cr (VI) with *Trichoderma viride* immobilized fungal biomass and cell free Ca-alginate beads, J. Exp. Biol. 45 (2007) 657–664.
[20] Y. Lai, G. Annadurai, F. Huang, J. Lee, Biosorption of Zn (II) on the different Ca-alginate beads from aqueous solution, Bioresour. Technol. 99 (2008) 6480–6487.
[21] C.C.V. Cruz, A.C.A. Da Costa, C.A. Henriques, A.S. Luna, Kinetic modeling and equilibrium studies during cadmium biosorption by dead *Sargassum sp.*, Biomass Bioresour. Technol. 91 (2004) 249–257.
[22] G. Yan, T. Viraraghavan, M. Chen, A new model for heavy metal removal in a biosorption column, Adsorpt. Sci. Technol. 19 (2001) 25–43.
[23] G. Bohart, E.Q. Adams, Some aspects of the behavior of charcoal with respect to chlorine, J. Am. Chem. Soc. 42 (1920) 523–544.
[24] R.A. Hutchins, New methods simplified design of activated carbon systems, Chem. Eng. Sci. 80 (1973) 133–138.
[25] D.C.K. Ko, J.F. Porter, G. McKay, Optimized correlations for the fixed bed adsorption of metal ions on bone char, Chem. Eng. Sci. 55 (2000) 5819–5829.
[26] D.O. Cooney, Adsorption Design for Wastewater Treatment, CRC Press, Boca Raton, 1999.